ChemComm

Cite this: *Chem. Commun.*, 2012, **48**, 6145–6147

www.rsc.org/chemcomm

COMMUNICATION

Organosilane micellization for direct encapsulation of hydrophobic quantum dots into silica beads with highly preserved fluorescence†

Liang Huang, Zhihui Luo and Heyou Han*

Received 22nd March 2012, Accepted 24th April 2012
DOI: 10.1039/c2cc32084c

Effective silica coating on hydrophobic quantum dots (QDs) was achieved by ultrasonic fragmentation of lipophilic silane–QDs precusor into water-soluble micelles and subsequent silicate deposition. This method allowed high retention of QD fluorescent properties and an easy scaling over the size and loading amount of silica beads.

Coating monodispersed and organically capped quantum dots (QDs) with a silica layer can greatly enhance their water dispersity toward biological use.[1] Particularly, this layer provided the inner QDs with robust colloidal and photochemical stability under physiological conditions, and reduced their cytotoxicity by blocking heavy metal release from the semiconductor core.[2] Conveniently, the thickness of this silica layer can be controlled well by established protocols[3] and desired surface functionalization can be achieved *via* silane coupling chemistry.

In general silica coating procedures, the lipophilic QDs have been rendered water-soluble to achieve a vitreophilic surface for silica monomer deposition in alkaline solution. 3-mercaptopropyl-trimethoxysilane (MPS)[4,5] and hydrolyzed tetraethyl orthosilicate (TEOS)[6] have been adopted to silanize the QD surface *via* ligand exchange prior to further silane condensation. Alternative routes have employed surfactants to solubilize QDs in water followed by templated growth of a mesoporous silica shell,[7] or silanization of the QD surface with organically modified trialkoxysilanes.[8] More conveniently, hydrophobic QDs have been simply incorporated into uniform-sized silica spheres by a reverse microemulsion approach.[9] There, a ligand exchange of QDs by hydrolyzed TEOS could explain their transport into the aqueous interior of the reverse micelle, accompanied by a drop in quantum yield.[9b] On the basis of fluorescence preservation, the encapsulation with alkyl-modified silane[8a] on a hydrophobic QD surface seemed particularly interesting, since it allowed a high retention of QD original capping ligands.

In this communication, a lipophilic interior in a silica bead was created for the direct incorporation of hydrophobic CdSe/ZnS QDs and also their fluorescence preservation. As illustrated in Scheme 1, the oil-soluble QDs were dissolved in a lipophilic silane (*n*-octyl triethoxy silane, OTES) and the oil phase was homogeneously emulsified in water by ultrasonication. The created nanometric emulsion droplets immediately transformed into water-soluble micelles, upon hydrolysis of siloxane groups of OTES into silanols under ammonia catalysis. Silicate was further deposited onto the silanol anchor points of the micelles to improve their colloidal and photochemical stability. As a novel silica coating strategy, we investigated the factors that dominate the morphology of the silica bead, the dynamics over the micelle evolution and the effect of silica coating on QD fluorescent properties.

The oil-soluble CdSe/ZnS QDs with an average diameter of 4.7 nm were used as the starting material (Fig. 1A). The QDs incorporating silica beads possessed mean diameters of 16.2 nm, 25.5 nm and 38.6 nm, which are illustrated in Fig. 1B–D, respectively. The formed silica beads exhibited a spherical shape with a multicore/shell structure and the morphology of a single QD in silica can be resolved in the Fig. 1 insets. The EDX result further confirmed the existing elements in CdSe/ZnS QDs and the silica shell (Fig. S1†). Simply in the current synthesis, the size and QDs loading amount of the silica beads were controlled by adjusting the mutual solubility of the oil (silane dissolving QDs) and water phases, using various QD concentrations in the silane precursor. Since OTES could be easily emulsified in water by ultrasonication without surfactant use, a low QD concentration (2.1×10^{-4} mol L^{-1}) facilitated the precursor to be shattered into smaller pieces (16.2 nm) by cavitation. With more QDs dissolved (6.4×10^{-4} mol L^{-1}), the dispersing ability of the silane precursor into the water phase was further reduced and the same energy input could create only less

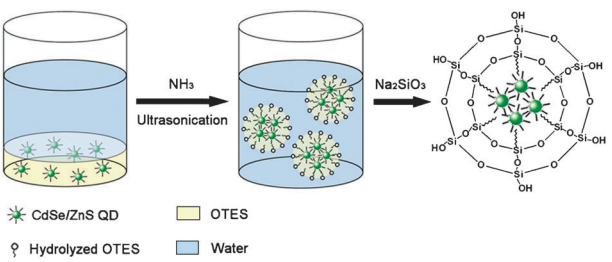

Scheme 1 Preparing stages of hydrophobic QDs embedded silica beads.

State Key Laboratory of Agricultural Microbiology, College of Science, Huazhong Agricultural University, Wuhan 430070, China. E-mail: hyhan@mail.hzau.edu.cn; Fax: +86-27-87288246; Tel: +86-27-87288246

† Electronic supplementary information (ESI) available. See DOI: 10.1039/c2cc32084c

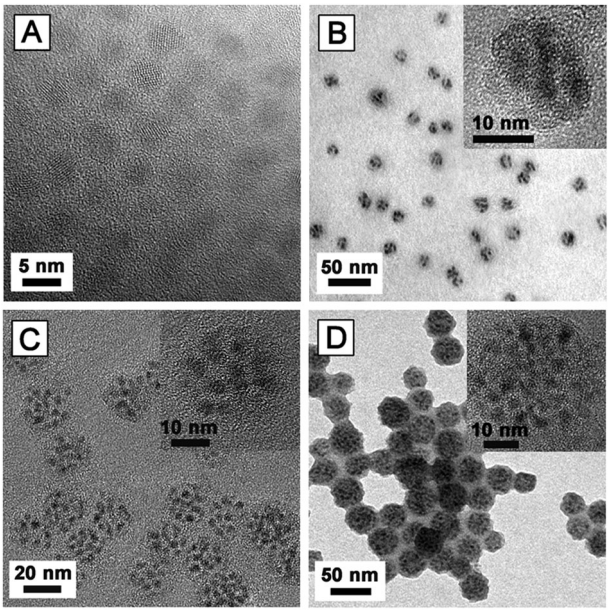

Fig. 1 TEM images of hydrophobic CdSe/ZnS QDs (A) and different sized silica beads encapsulating multiple QDs: 16.2 nm (B), 25.5 nm (C) and 38.6 nm (D). The inset shows the magnification of a single silica bead.

interfacial area of the two phases, leading to larger droplets (38.6 nm) with more QDs entrapped. Noticeably, this scaling over the bead size should be taken within a certain QD concentration range. For example, with a large excess of QDs applied (1.1×10^{-3} mol L^{-1}), aggregates of the nanocrystals appeared (Fig. S2†), since the silane precursor was inadequate for an effective emulsification. At the other extreme, a rather low QD concentration (4×10^{-5} mol L^{-1}) caused only an irregular and amorphous silica structure (Fig. S2†). This phenomenon could be partially explained by the stabilizing effect of the entrapped insoluble lipids (QDs in this case) to the oil in water emulsion droplets.[10]

To understand the dynamics over the silica bead (25 nm) formation, the hydrodynamic diameters (HD) of the micelles were monitored by dynamic light scattering. As indicated in Fig. 2A, the newly created emulsion droplets (82 nm) showed a minimizing of HD down to 40 nm in the ultrasonication stage, accompanied by a decrease in size distribution (Fig. 2A inset). The microemulsion appearance also indicated such a size decrement since it became more transparent along with the ultrasonication (Fig. S3†). This tendency could be ascribed to the gradual hydrolysis of OTES, producing more detergent-like silane species to stabilize finely dispersed micelles. Without ammonia catalysis, the solution remained turbid and the silane finally separated out from water as an immiscible phase when sonicating was stopped. This clearly indicated that the hydrolyzed OTES greatly contributed to the micellization. However, the newly created micelles proved to be dynamically unstable and coalesced after storage, resulting in an increased HD (Fig. 2A). To solve this problem, sodium silicate was introduced and slowly polymerized on the micelle silanol groups, which caused a small increment in micelle size and a stable size distribution (Fig. 2B). Visibly, the silicate deposited micelles showed little size variation after ten days storage, indicating

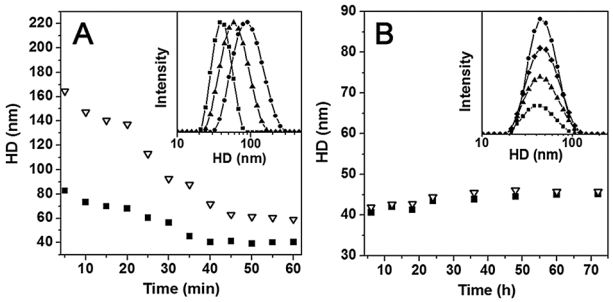

Fig. 2 The evolution of micelle hydrodynamic diameter in the ultrasonication stage (A) and silicate deposition stage (B) measured right after synthesis (squares) and in ten days storage (triangles). Insets: micelle size distribution after ultrasonication for 5 min, 25 min and 40 min (right to left in A) and silicate deposition for 0 h, 24 h, 48 h and 72 h (bottom to top in B).

the colloidal stability was greatly enhanced by this silica shelling (Fig. 2B). The final hydrated size of the beads (45 nm) was larger than their dry size (25 nm) measured by TEM, which was possibly caused by the electrical bilayer of the charged silica beads in water.

The micelle evolution in the whole synthesis was directly visualized by TEM. It was found that the extent of silicate deposition determined the final morphology of the micelles. As revealed in Fig. S4†, the new silane–QDs micelles created by ultrasonication showed a high tendency to coalesce. When deposited with silicate, the micelles evolved gradually from a deformable structure to spherical beads. In the control experiment, the micelles without further silicate "shaping" were almost irregularly shaped and prone to coalesce on the TEM grid. Obviously, this trend in micelle coalescing was effectively suppressed by silica shelling, which can explain the enhanced colloidal stability observed above well.

For QD silication, a big challenge that remains is preserving their original optical properties, since they are highly sensitive to the surface capping. In the current method, we observed a reversible change in the photoluminescence quantum yield (PL QY) of incorporated QDs along with the coating. The QDs in chloroform had a PL QY estimated to be 50%, which was reduced by nearly half in the silane micellization stage (Fig. 3A). The following silicate deposition gradually increased the QY up to 90% of the initial value (45% relative to 50%) after 72 h reaction (Fig. 3B). To confirm this change, time-resolved photoluminescence of the micelles was measured at different synthetic stages (Fig. 4A). The PL decay curves of

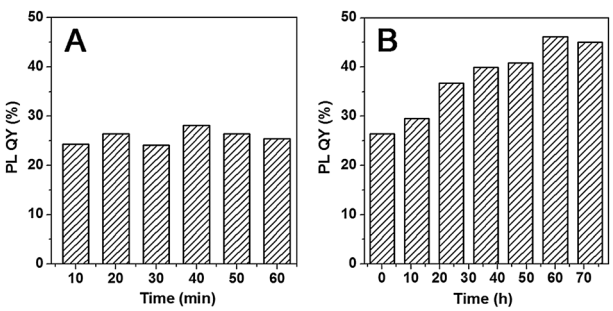

Fig. 3 PL QY of incorporated QDs in the ultrasonication (A) and silicate deposition (B) stages.

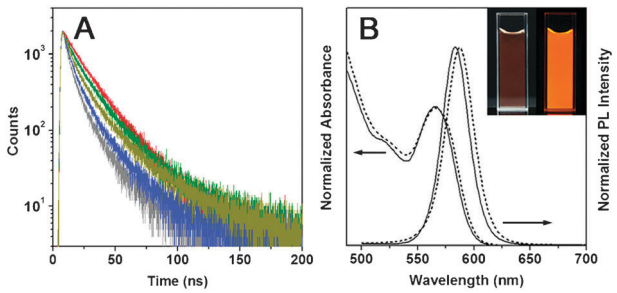

Fig. 4 (A) Fluorescence decay curves of CdSe/ZnS QDs at different synthetic stages: (bottom to top) ultrasonicated for 40 min, deposited with silicate for 24 h, 48 h, 72 h and before encapsulation (in chloroform). (B) Absorption and PL spectra of CdSe/ZnS QDs before (solid line) and after (dashed line) silica coating. Inset: photographs of QDs/SiO_2 nanobeads in water under daylight (left) and UV lamp (right).

both oil-soluble and silica-coated QDs can be fitted to a biexponential model and the fitting parameters are listed in Table S1†. The PL decay became faster in the ultrasonication stage with the mean lifetime decreased from the initial 20.77 ns to 16.80 ns. As the silica shell formed, the mean lifetime gradually recovered and reached 23.27 ns after 72 h deposition. Meanwhile, a decreased slow decay component, which would be associated with the surface-related QD emission, was observed and this was possibly caused by the environmental change around QDs and potential QD surface modification by the silica species.[9b] Clearly, the recovering behavior in PL lifetime, together with that in PL QY indicates that the phase dispersion caused impermanent PL degrading on the QDs, possibly originating from the increased solvent polarity, as well as the diffusion of oxygen and water molecules onto the QD surface.[8b] The PL performance was enhanced by the deposited silica layer, implying an effective protection of the QD surface from the external polar environment.

The absorption and fluorescence spectra of the water-soluble QDs/SiO_2 nanobeads exhibited the same profiles as those of the hydrophobic QDs (Fig. 4B). The silica shell growth dramatically improved the PL stability of incorporated QDs. As demonstrated in Fig. S5†, the micelles after 72 h silicate deposition showed little PL degradation in 1 × TBE (Tris–borate–EDTA) buffer when excited continuously for 1 h. In contrast, the uncoated micelles were partially quenched and a severe quenching was observed for mercaptopropionic acid-capped CdSe/ZnS QDs under the same conditions.

Based on the fluorescent beads, extensive silica coatings may favor the integration of additional functionalities into the beads by stepwise assembly.[11] Here, we demonstrated the seeded growth of the nanobeads (25 nm) in an ethanol/water (3 : 1) mixture using TEOS as the silica monomer. Fig. 5 shows that the nanospheres consisted of an organosilica core (brighter) with multiple QDs and a 15 nm silica shell (darker). The distinguishable core/shell structure indicates that the QDs were most probably located in a less dense hydrophobic region of the silica sphere. As revealed in Fig. S6†, the QDs/SiO_2 beads retained most of their original emission characters after this additional silica coating. The thickness of this silica shell can be controlled by the well-known Stöber process.[3a] It is noteworthy that the initial thin silica layer was important to shield the micelles from flocculation when transferred into the ethanol/water mixture, considering the reduced interparticle electrostatic repulsion in a low polar environment.[3b]

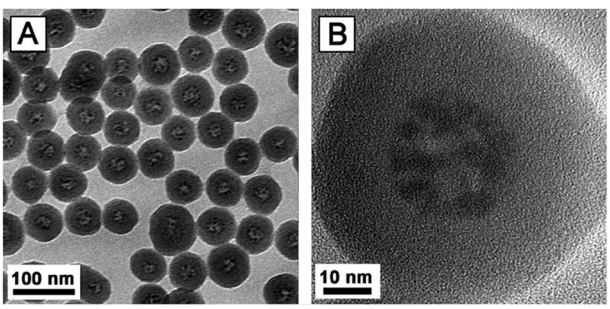

Fig. 5 (A) A TEM image of 25 nm nanobeads coated with a 15 nm thick silica shell. (B) An enlarged image of a single silica nanosphere.

In summary, we demonstrated a novel and effective silica coating on hydrophobic QDs based on organosilane micellization and silicate deposition. This method skipped the conventional water solubilization step for oil-soluble QDs and greatly favored the fluorescence preservation by confining the QDs in a lipophilic interior of a silica bead. The facile ultrasonic fragmentation of organosilane precursor enabled an easy scaling over silica bead size and the loading amount of hydrophobic contents, which is especially favorable for a compact loading of desired nanocrystals in silica for signal amplification. Considering the enhanced brightness over a single QD in a silica sphere and good photostability in aqueous media, the nanobeads are suited to sensitive fluorescent labeling in biological research.

The authors gratefully acknowledge the financial support for this research from National Natural Science Foundation of China (20975042, 21175051), the Fundamental Research Funds for the Central Universities (2010PY009, 2010PY139) and the Natural Science Foundation of Hubei Province Innovation Team (2011CDA115).

Notes and references

1 M. Bruchez Jr., M. Moronne, P. Gin, S. Weiss and A. P. Alivisatos, *Science*, 1998, **281**, 2013.
2 C. Kirchner, T. Liedl, S. Kudera, T. Pellegrino, A. M. Javier, H. E. Gaub, S. Stölzle, N. Fertig and W. J. Parak, *Nano Lett.*, 2005, **5**, 331.
3 (*a*) W. Stöber, A. Fink and E. Bohn, *J. Colloid Interface Sci.*, 1968, **26**, 62; (*b*) L. M. Liz-Marzán, M. Giersig and P. Mulvaney, *Langmuir*, 1996, **12**, 4329.
4 D. Gerion, F. Pinaud, S. C. Williams, W. J. Parak, D. Zanchet, S. Weiss and A. P. Alivisatos, *J. Phys. Chem. B*, 2001, **105**, 8861.
5 T. Nann and P. Mulvaney, *Angew. Chem., Int. Ed.*, 2004, **43**, 5393.
6 P. Yang, M. Ando and N. Murase, *Langmuir*, 2011, **27**, 9535.
7 (*a*) I. Gorelikov and N. Matsuura, *Nano Lett.*, 2008, **8**, 369; (*b*) X. G. Hu, P. Zrazhevskiy and X. H. Gao, *Ann. Biomed. Eng.*, 2009, **37**, 1960.
8 (*a*) Z. Zhelev, H. Ohba and R. Bakalova, *J. Am. Chem. Soc.*, 2006, **128**, 6324; (*b*) R. C. Han, M. Yu, Q. Zheng, L. J. Wang, Y. K. Hong and Y. L. Sha, *Langmuir*, 2009, **25**, 12250.
9 (*a*) M. Darbandi, R. Thomann and T. Nann, *Chem. Mater.*, 2005, **17**, 5720; (*b*) R. Koole, M. M. Schooneveld, J. Hilhorst, C. M. Donegá, D. C. Hart, A. Blaaderen, D. Vanmaekelbergh and A. Meijerink, *Chem. Mater.*, 2008, **20**, 2503.
10 T. Delmas, H. Piraux, A. C. Couffin, I. Texier, F. Vinet, P. Poulin, M. E. Cates and J. Bibette, *Langmuir*, 2011, **27**, 1683.
11 Y. Piao, A. Burns, J. Kim, U. Wiesner and T. Hyeon, *Adv. Funct. Mater.*, 2008, **18**, 3745.